Influence of Cu grain size on running-in related phenomena

D. Shakhvorostov [a,1] L. Jian [b] E. Nold [c] G. Beuchle [d] M. Scherge [a]

[a] *IAVF Antriebstechnik AG, Im Schlehert 32, D-76187 Karlsruhe, Germany*

[b] *Wuhan Research Institute of Materials Protection CAMST, 126 Bao Feng Erlu, Wuhan, China*

[c] *Institut für Materialforschung IMF I Forschungszentrum Karlsruhe GmbH Hermann-von-Helmholtz-Platz 1, D-76344 Eggenstein-Leopoldshafen, Germany*

[d] *Institut für Technische Chemie ITC-TAB Forschungszentrum Karlsruhe GmbH Hermann-von-Helmholtz-Platz 1, D-76344 Eggenstein-Leopoldshafen, Germany*

Abstract

We used a single-asperity microscopic tribosystem diamond sphere / Cu sheet to investigate the relevant phenomena affecting the dynamics of friction and wear in a macroscopic system. The influence of the average grain size of the softer of two tribopartners on friction and wear was investigated in particular. The observed tribosystem experienced a natural transition during the running time, from severe plastic flow to predominating boundary lubrication. This fact was used to study the influence of poly-α-olefine base oil and fully formulated engine oil Fuchs Titan SAE 5W45 on friction and wear during severe deformation and boundary lubrication regime. It is shown that the initial grain size has a crucial influence on wear and friction only during first sliding interactions. During the initial sliding the grain size rapidly decreases due to plastic deformation and achieves a nearly equal value for every initial situation after approximately 30 cycles. Initially larger grains result in increased friction and wear as well as higher sensitivity to the kind of lubrication.

Key words: running-in, grain size, friction, wear

Email addresses: dshakhvo@uwo.ca (D. Shakhvorostov), matthias.scherge@iavf.de (M. Scherge).

URL: www.iavf.de (M. Scherge).

[1] *Present adress: Department of Applied Mathematics, University of Western Ontario, London, Ontario N6A 5B7, Canada*

1 Introduction

Friction and wear in a macroscopic tribosystem depend upon many parameters (e.g. maximum contact pressure, contact temperature), which vary with respect to sliding velocity, load, and running time. The time dependence of wear and friction without external changes of load or sliding velocity implies internal changes inside the tribosystem with respect to topography, mechanical properties and the ability to provide boundary lubrication. Intensive changes usually happen during first seconds to hours of the system run time, which is known as running-in [1–3]. Sliding induced changes during running-in may affect the tribosystem in its later operating time, for instance double its service life [4]. Although it is known that microstructure and chemistry of the surface affect the friction and wear, strong influence of running-in on later operating time is not yet completely understood. Using molecular-mechanistic approach on friction and wear as described in [1,2] it could be shown how mechanical properties and shear strengths on tribological junctions might influence friction and wear. Unfortunately this approach is unable to predict neither mechanical properties or shear strengths. Computational methods applied to friction problems are more flexible and can access structural and chemical changes inside the contact during friction, although having limitations on the size and time scale of the systems studied. Experimental studies thus remain, as ever, the correct and affordable information source about the frictional changes as running-in is the most suitable period to study them.

There are several types of running-in or break-in [5] classified depending on the nature of transition, categorized as to how friction and wear vary during run time. As for oil lubricated systems the decrease of friction and wear rate occurs due to a decrease of plastic flow in the original material and the formation of dissipative structures. Running-in is accompanied by a change of topography and morphology that can be measured as decrease or increase of roughness [1,4]. Dissipative structures imply a formation of complex layered structure often consisting of deformed, highly deformed, nanocrystalline layers and anti-wear films. Deformed layers in a tribological contact appear in workhardening metals [6] separating bulk and highly deformed layer. Deformed layers have increased hardness in comparison to the bulk. Properties of highly deformed surface layers, as described in [7–13], are sometimes affected by inclusions of anti-wear agents, oxides etc. In general they posses significantly reduced grain size, texture with respect to the sliding direction and residual stresses influencing the choice of favorable slip systems during plastic deformation. In case of layers with an average grain size below 10-100 nm the deformation behavior might change significantly and such layers can act quasi superplastically, exhibiting low shear strength at high strain rates [14–16]. First studies of friction on single crystals have shown a strong dependence of the friction on the orientation of sliding with respect to the crystallographic orientation, as long as no friction induced texture have appeared yet. In a many-asperity macroscopic contact, deformed layers, as obtained from single pass interaction, have independently from initial orientation of single crystals a texture, where cells might have {110} plane facing the surface [17]. From friction experiments on many-asperity contacts, it is known that around 500 passes are necessary in order to induce the steady-state friction coefficient and texture [5]. Although texture and appearance of the deformed layers are studied well there is little information about the dynamics of their formation for a single asperity contact, that is of high significance for the modeling of friction and wear. This study shall provide additional information about the morphology of the deformed layers as appearing in a single asperity interaction, and especially about the dynamics of formation of the deformed layer in a well defined contact geometry. Following aspects are to be studied as function of sliding interactions:

(1) microstructure, e.g. the grain size of the near surface material, influence of the lubricant on morphology and
(2) chemistry, e.g. the changes of elemental composition affected by lubricant with and without anti-wear agents and dispersants.

We use coarse-grained and fine-grained starting material in order to investigate the significance of starting structure for the near surface material deformation dynamics. Previous studies [18,19] have already shown that reducing the grain size of material in the initial state leads to improved stability of the tribosystem and to a decrease of wear and friction. In a real macroscopic contact grain size could decrease due to plastic flow and increase due to recrystallization at higher temperatures. In our tribosystem we expect only the reduction of grain size, because no high temperatures are assumed to occur in the contact. Using a plane base and a fully formulated oil, we expect to receive information about the influence of additives on grain size evolution as we minimize hydrodynamic effects by setting a low sliding velocity. The ball-on-plane geometry provides good basis for later simulation as well as high stability of the contact area. In addition, ideally hard sphere and ideally plastic flat surface help to estimate the real contact area during first sliding interactions.

2 Experimental details

2.1 Sample preparation and characterization

Our tribopartners consisted of materials with well-defined chemical and structural properties, where oxygen-free copper of 99.9 mass percent purity was used. Most impurities were P<0.012% and S<0.001%. Square samples 10×7

mm^2, one sample for each sliding condition, were cut from a cold-rolled and annealed sheet of 1.5 mm thickness with an average grain size of about 3 μm. The nanohardness of the samples was about 1.5 GPa and Young's modulus was approximately 130 GPa. This sample set was called "sample 3 μm". In order to induce secondary recrystallization, a Cu sheet was for 10 hours annealed at 950 ℃ under a 10^{-6} mbar (10^{-4} Pa) vacuum. After this procedure, the average grain size increased to about 2 mm (sample 2 mm). The nanohardness of these samples was approximately 1 GPa and their Young's modulus about 120 GPa. Both sample sets were polished and then electropolished.

2.2 Friction tests

A reciprocating microtribometer Tetra [20] was used to create the wear tracks. The microtribometer consed of a combination of precision drives – a force transducer made of steel and a fiber-optical length detection system to measure the deflections of the force transducer (see Fig. 1).

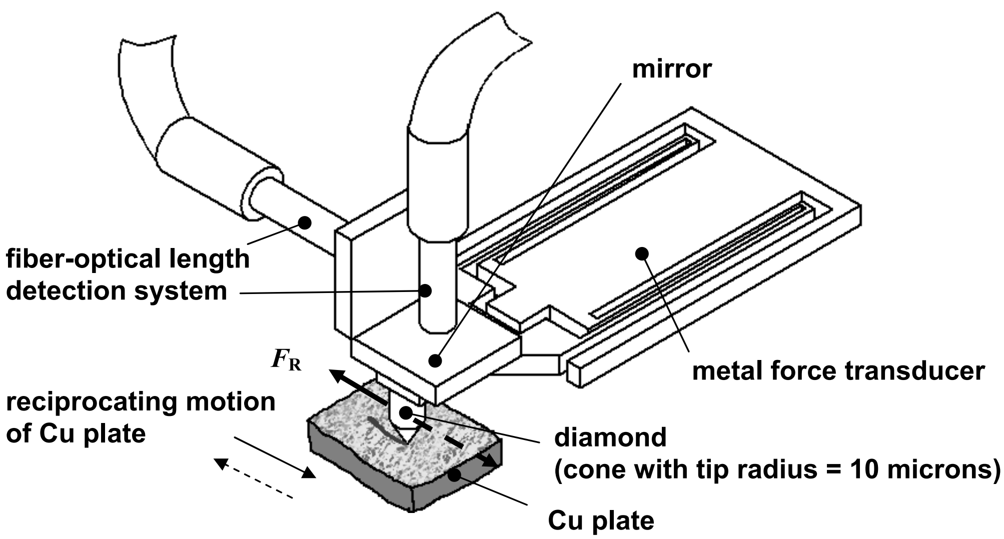

Fig. 1. Microtester setup for friction measurements.

During all test sets, sliding conditions as defined by normal load, sliding velocity, sliding length, temperature, and relative humidity were kept constant. To be specific, during the tests, the velocity and normal force were kept constant at 130 μm/s and 6 mN, respectively. The linearity of the sliding velocity is given at 80 of the track length, so that the latter microstructure analysis is done in the middle of the tracks. In order to determine wear as a function of time, 6 tracks with 1, 5, 30, 50, 100, and 200 reciprocations (cycles), respectively were created with a spherical diamond tip (10 μm radius) in a Cu sheet for each microstructure and type of lubrication. The length of the track was about 700 μm. The friction tests were performed at 25°C and 60% relative humidity. First, the tests without lubrication, afterwards the tests with a poly-α-olefine base oil lubrication, and finally, tests with synthetic engine oil lubrication Fuchs Titan Supersin SL(SAE 5W40, additive packages containing less than one weight percent of Ca, Zn, P, S as well as N and Cl as trace elements) were carried out. In order to reduce contamination, the diamond tip was cleaned by indentation in Cu before each test. The coefficient of friction was averaged over the sliding distance during each cycle.

2.3 Wear measurements

The geometries of the wear tracks were analyzed by atomic force microscopy immediately after the friction test. The estimated track depths were in the range of 100 nm to 3 μm. For each wear mode, the ratio of material removed from the surface to material transferred to the shoulders of the wear track was determined [21,22]. This ratio is expressed as parameter β_{HK} as defined in Eq. (1) and Fig. 2:

$$\beta_{\mathrm{HK}} = \frac{A_2 - A_1}{A_2}. \qquad (1)$$

In the ploughing mode, all material is transferred from the groove to the shoulders ($\beta_{\mathrm{HK}} = 0$). Here, no volume loss and, hence, no wear occurs. Wear is defined as the difference $A_2 - A_1$. For the wedge formation mode, the value is in the range $0.2 < \beta_{\mathrm{HK}} < 0.8$. In the cutting mode, it is in the range $0.8 < \beta_{\mathrm{HK}} < 0.95$.

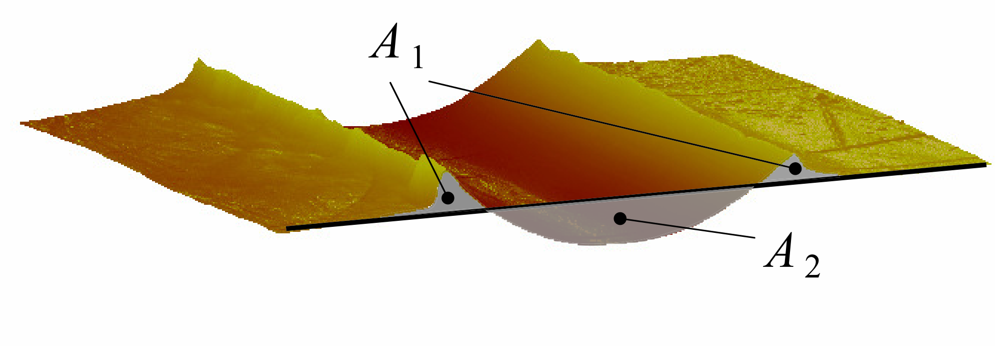

Fig. 2. Atomic force microscope image of a wear groove.

2.4 (AES) Auger spectroscopy and electron microscopy

To analyze the elemental composition of the surfaces the AES measurements [23] were performed using a PHI 680 Auger Nanoprobe system with a base pressure in the analysis chamber less than 10^{-9} mbar. For AES measurements the primary beam energy was set either to $E_{\mathrm{p}} = 10$ kV or to 20 kV. The primary current was kept at $I_{\mathrm{p}} = 20$ nA for profiles and spectra, and at $I_{\mathrm{p}} = 10$ nA for SEM images. The angle of incidence of the primary electron beam was 30° to the sample surface. In order to minimize the influence of the electron radiation on chemistry of the sample, the profiles were recorded in the scanned mode over an area of 2×2 μm^2. The beam size of the primary electron beam was <20 nm.

The energy resolution of the cylindrical mirror analyzer is fixed at $\frac{\Delta E}{E} = 0.6\%$ for the kinetic energy of the Auger electrons. The following Auger transitions were used for Auger depth profiles: Cu = 922 eV, Ca = 297 eV, Zn = 997 eV, S = 150 eV, and C = 175 eV.

Quantification was usually performed empirically by the use of standards with known composition. In order to obtain depth profiles, the samples were etched by a differentially pumped ion gun under the following conditions: 2 kV Ar^+-ions, $I = 500$ nA, scanning area 2×2 mm^2, incidence angle 45°. Standard for depth calibration was 100 nm thick SiO_2 layer on Si. Data processing [24] was carried out with PHI's "Multipak Version 7.3A" software that is based on Matlab.

2.5 (EBSD) Electron backscatter diffraction

To analyze the orientation of the Cu grains the electron backscatter diffraction (EBSD) was used. Backscatter diffraction pattern were obtained in an environmental scanning electron microscope (ESEM) XL30 FEG under high vacuum conditions, 10 kV accelerating voltage and 100 μm aperture. The EBSD-System made by TSL, was calibrated with a Nickel-standard. Analysis of crystal orientation was performed on wear track areas of approximately 3×12 μm^2 with a step size of 0.2 μm.

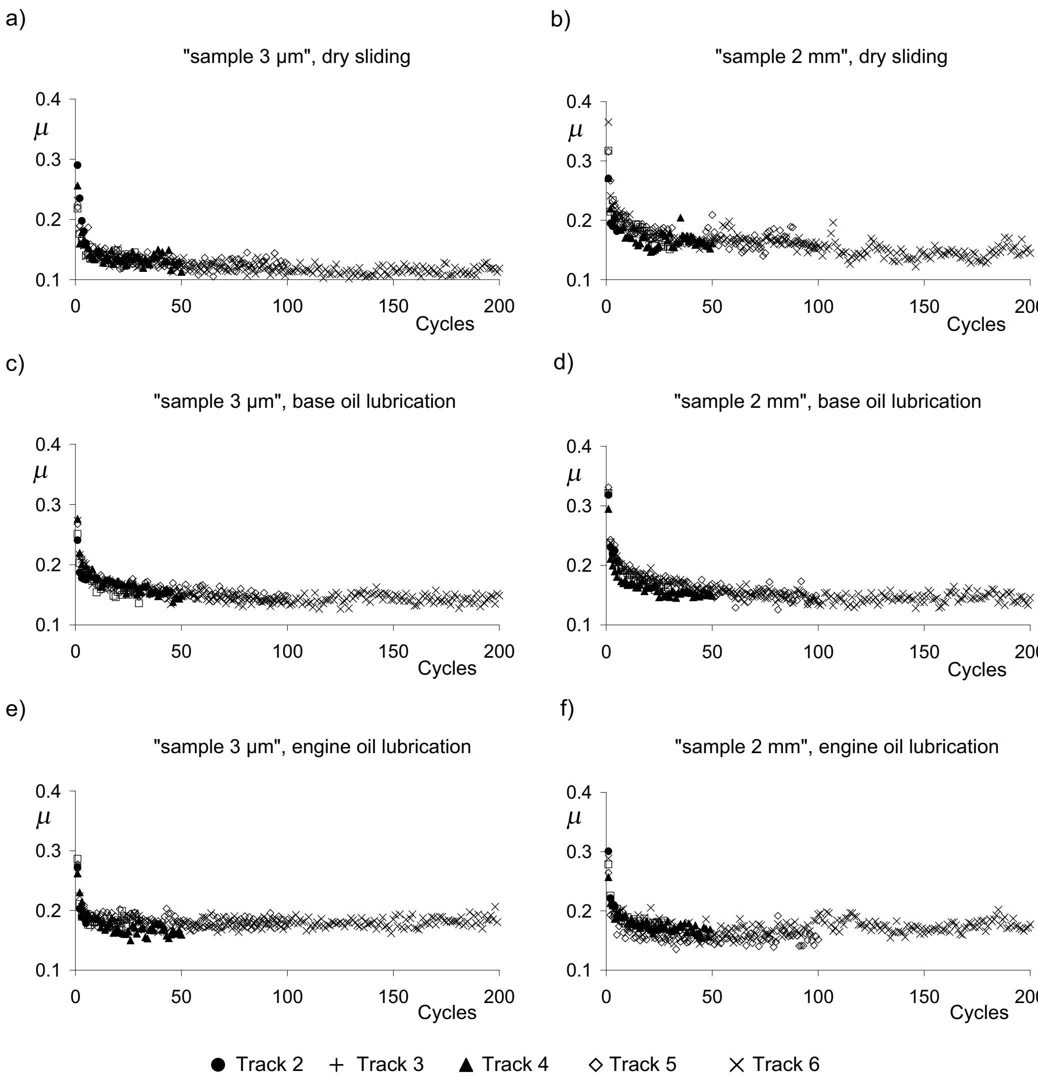

Fig. 3. Coefficient of friction as a function of cycles.

3 Results

3.1 Friction

One of the central interests in this work is to investigate how the friction in our trybosystem changes with time. This section deals with results of friction measurement and explains a common for all sliding situations characteristic behaviour. The diagrams in Fig. 3 summarize the results. The coefficient of friction μ is shown as a function of cycles (reciprocations) under dry and lubricated sliding conditions. Each point represents a mean value during one cycle. In all experiments sliding took place without stick-slip. Under all sliding conditions, the following characteristics are obtained: during the first cycle, μ

is maximum, within the range of 0.25 - 0.32. During the next cycles, μ drops exponentially fast to a nearly constant value (0.13 for dry sliding, 0.15 for base oil lubrication, and 0.18 for engine oil lubrication) after 50 cycles with a time constant of 10 to 20 cycles. The following two phases are indicated in the curve: 1 – very first cycles with dropping μ and 2 – a section after 50 cycles with nearly constant μ.

Under dry sliding conditions the average value of μ and its fluctuations are higher for "sample 2 mm" than for "sample 3 μm", as shown in Figs. 3 a and b. The reason for this significant difference is the brittle destruction of the natural oxide layer on the copper "sample 2 mm" by diamond sphere, which happens under dry sliding only. Under lubrication, μ decreases (see 3 c, d, e, and f) slightly less during the first cycles as compared to the dry friction case. In the second phase after 50 cycles, however, the average steady-state value of μ increases dependending on the type of oil. Differences between the lubricated "sample 2 mm" and the "sample 3 μm" were observed in the first cycle only ("sample 3 μm": 0.28 and "sample 2 mm": 0.29 - 0.31).

3.2 Wear

In our experiments, wear is strongly correlated with friction. In analogy to the friction, there are two phases of wear as a function of cycles (reciprocations) under all sliding conditions: 1 – wear increases rapidly during the very first cycles and 2 – after about 50 cycles, the wear rate remains almost constant and low. Details are shown in the diagram of Fig. 4 where each point corresponds to a mean value of area A_2 or ratio β_{HK} along the 100 μm wear track length.

Under all sliding conditions, "sample 3 μm" exhibits less wear than "sample 2 mm". However, the wear rates during phase 2 are nearly similar in both samples. The ratio β_{HK} is in the range of 0.6-0.8 (wedge formation) after the first cycle and decreases to 0.1 (ploughing) for "sample 3 μm" (see Figs. 4 a, c, and e), to 0.2 (ploughing - wedge formation) for "sample 2 mm" under dry sliding (Fig. 4 b) and to 0.4 (wedge formation) under lubricated sliding as shown in Figs. 4 d and f.

3.3 (SEM) Scanning electron microscopy of surfaces

Electron microscopy images (see Figs. 5 and 6) reveal the structural changes in the wear tracks. The initial structure of Cu changes immediately after first sliding interaction and keep changing for several cycles. At the end of experiment, the microstructure does not seem to depend on the initial state. The figures show the wear tracks of samples lubricated with engine oil, where

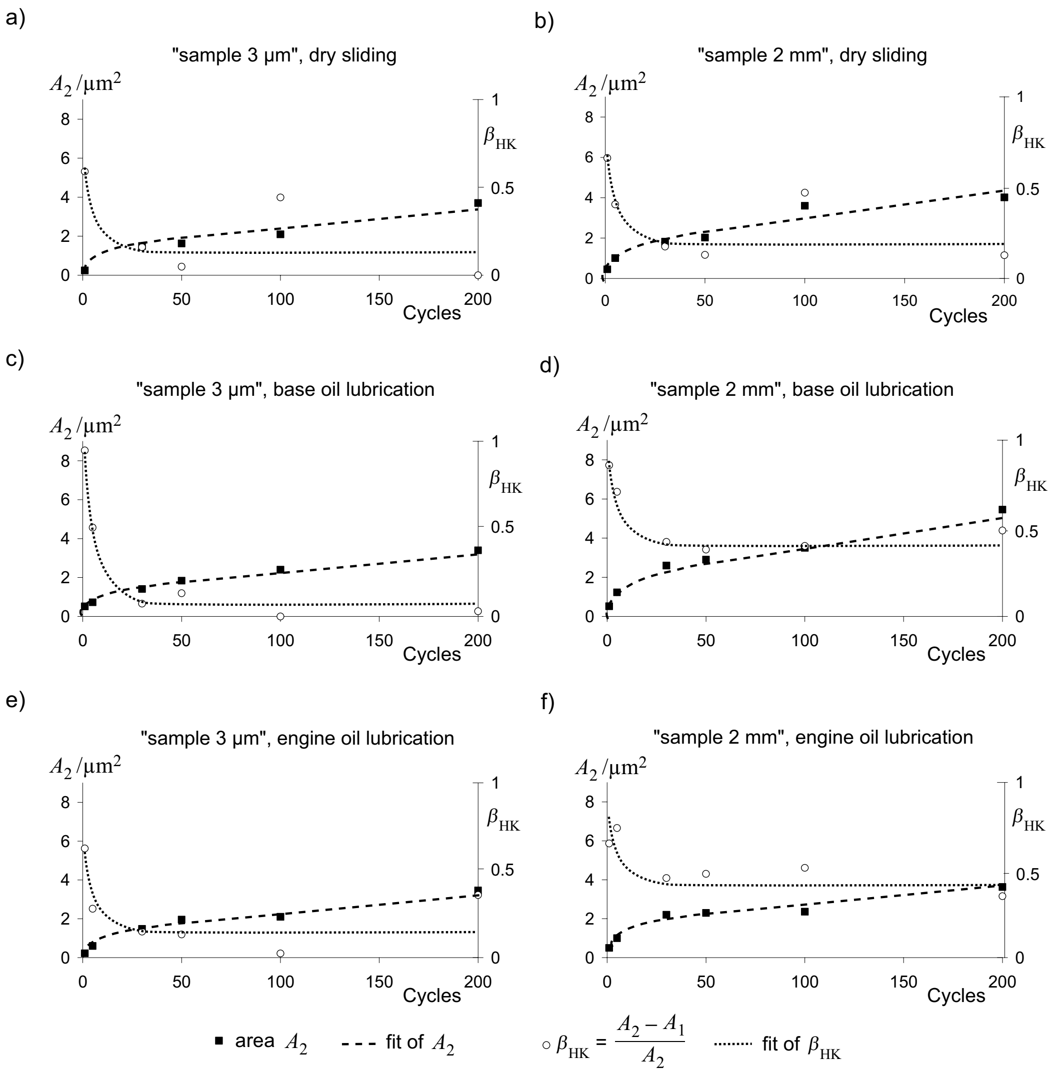

Fig. 4. Area A_2 and ratio β_{HK} as a function of cycles. Wear is a product of $\beta_{\mathrm{HK}} \cdot A_2$.

the typical grains are highlighted. Similar grain sizes were obtained on samples with base oil lubrication and dry friction (not shown).

After the first cycle, the initial microstructure of "sample 3 µm" has changed already, as is shown in Fig. 5 a. The grain size decreases until the 50th cycle (Figs. 5 b, c, and d). After 50 cycles, the grain size remains essentially constant with typical linear dimension of 500 nm. The grain boundaries become more clearly visible, as is shown in Figs. 5 e and f.

Sliding changes the grain size of "sample 2 mm" in a similar way, which initially seems to behave like a single crystal due to the large grain size. The diamond sphere generates several slip bands along the wear groove (Figs. 6 a and b). After 30 cycles, grains with different orientations appear (Fig. 6 c) with an average size of nearly 600 nm as on "sample 3 µm". After 50 cycles, the grain

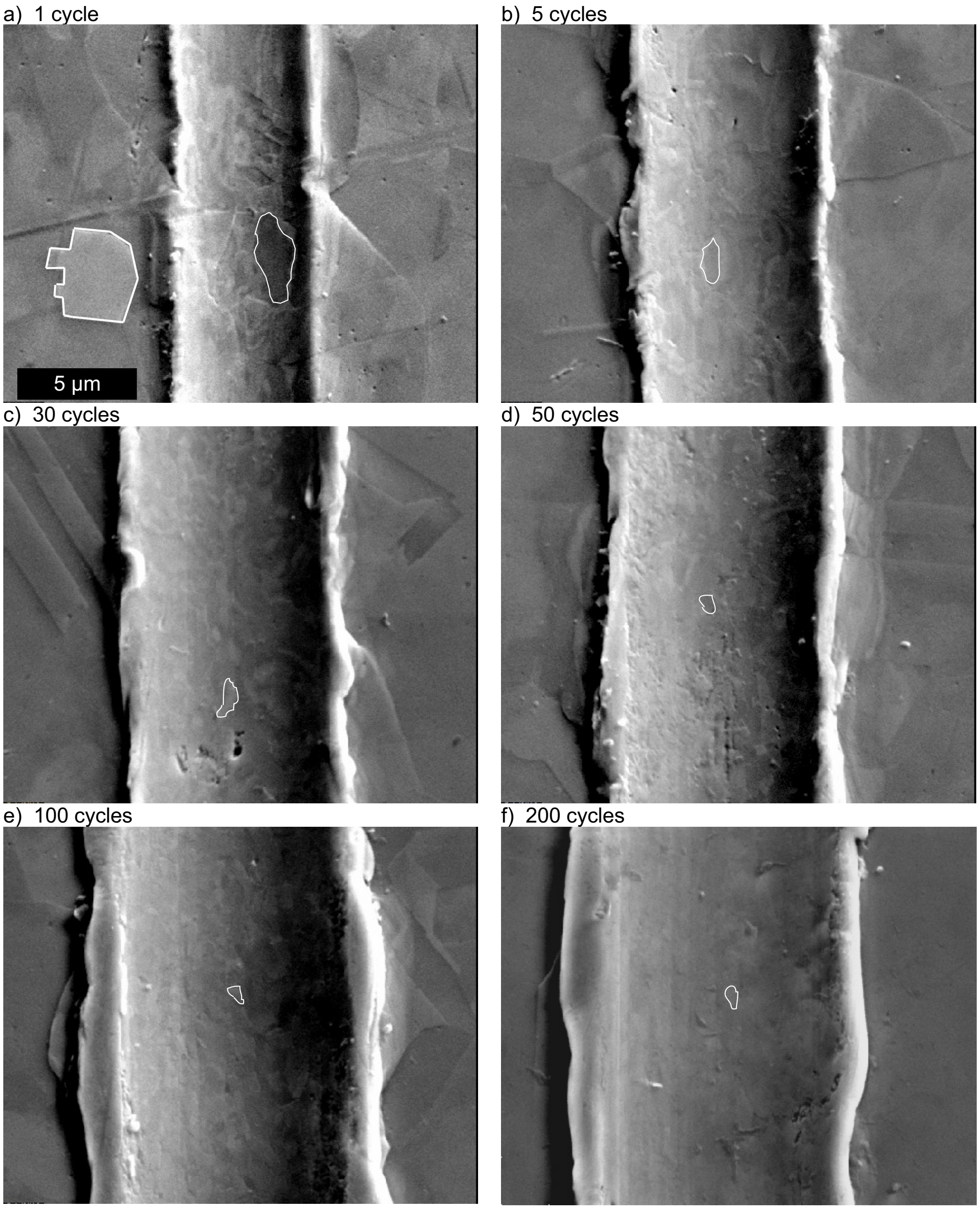

Fig. 5. Secondary electron micrographs of wear tracks of "sample 3 μm" lubricated with engine oil. One typical grain is highlighted in each panel.

size is not reduced any further, see Figs. 6 d, e and f. The grain boundaries become more clearly visible, similar to "sample 3 μm".

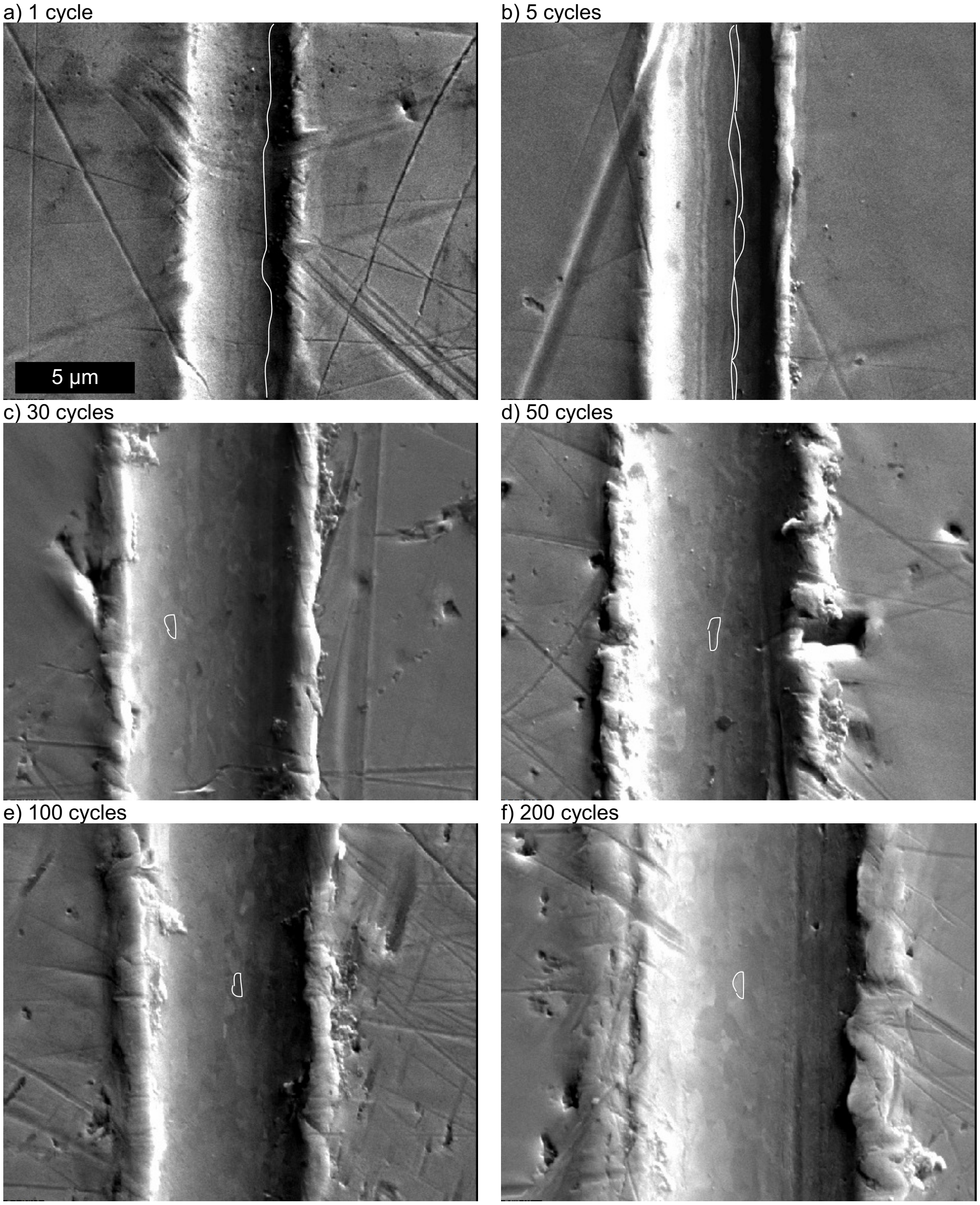

Fig. 6. Secondary electron micrographs of wear tracks of ”sample 2 mm” lubricated with engine oil. One typical grain is highlighted in each panel.

3.4 (EBSD) Electron backscatter diffraction on wear tracks

Electron backscatter diffraction defines the texture of the surface by revealing the orientation of crystalline planes and boundaries of grains. This information obtained from our samples show an induced texture after first sliding interaction, followed by slight recrystallization. The lubricated with engine oil "sample 3 μm" after 50 cycles, as can be seen in Fig. 7 a, shows a texture with a dominant plane (001) of the copper grains, which is oriented parallel to sliding interface. After 100 cycles, light recrystallization occurs, the reorientation of the grains takes place, as shown by Fig. 7 b. The shape of the grains is less extended in sliding direction and less texture appears after 200 cycles, see Fig. 7 c.

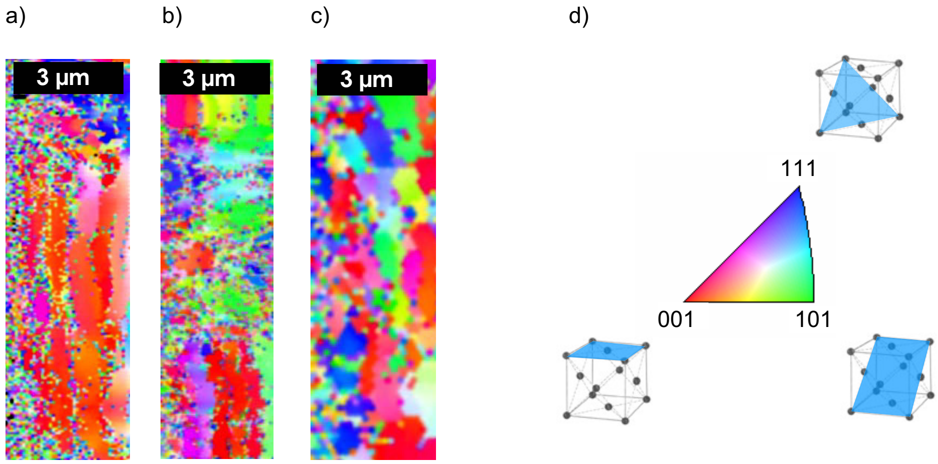

Fig. 7. EBSD analysis of wear tracks of "sample 3 μm" lubricated with engine oil, (a) shows the groove after 50 cycles, (b) after 100, and (c) after 200 cycles. The color scale of the orientation of fcc crystal planes is depicted in (d).

3.5 (AES) Auger electron spectroscopy atomic concentration depth profiles

In order to obtain the changes of atomic composition of near-surface regions during the friction process, Auger electron spectroscopy is applied to wear tracks and areas next to them. Fig. 8 shows the distribution of oxygen depending on cycles and sputter depth. Cycle 0 is the initial state of the surface. "Sample 2 mm" has slightly more oxygen on the surface in initial state than "sample 3 μm". This underlines that "sample 2 mm" originally has a continuous and/or thicker oxide layer than "sample 3 μm".

The oxygen concentration on the surface and in the solid increases during the friction process both without lubrication and with base oil lubrication (see Figs. 8 a-d). Also the depth of oxidation increases from 3-5 nm to nearly 8 nm. Less tribooxidation is observed for samples lubricated with engine oil, as is shown by Figs. 8 e and f. The oxidation depth remains nearly the same in both samples. Figures 9, 10, and 11 show the concentration profiles of elements relevant to engine oil lubrication (Ca, Zn, and S). In the initial state, none of these elements exist in the surface regions. After the friction process, the concentration changes as much as the depth. It is common to the concentration profiles of all elements that the concentrations as well as the depth of modification are nearly linearly dependent on the cycles. The initial structure of the samples does not have a clearly detectable influence on the changes of the concentration depth profiles.

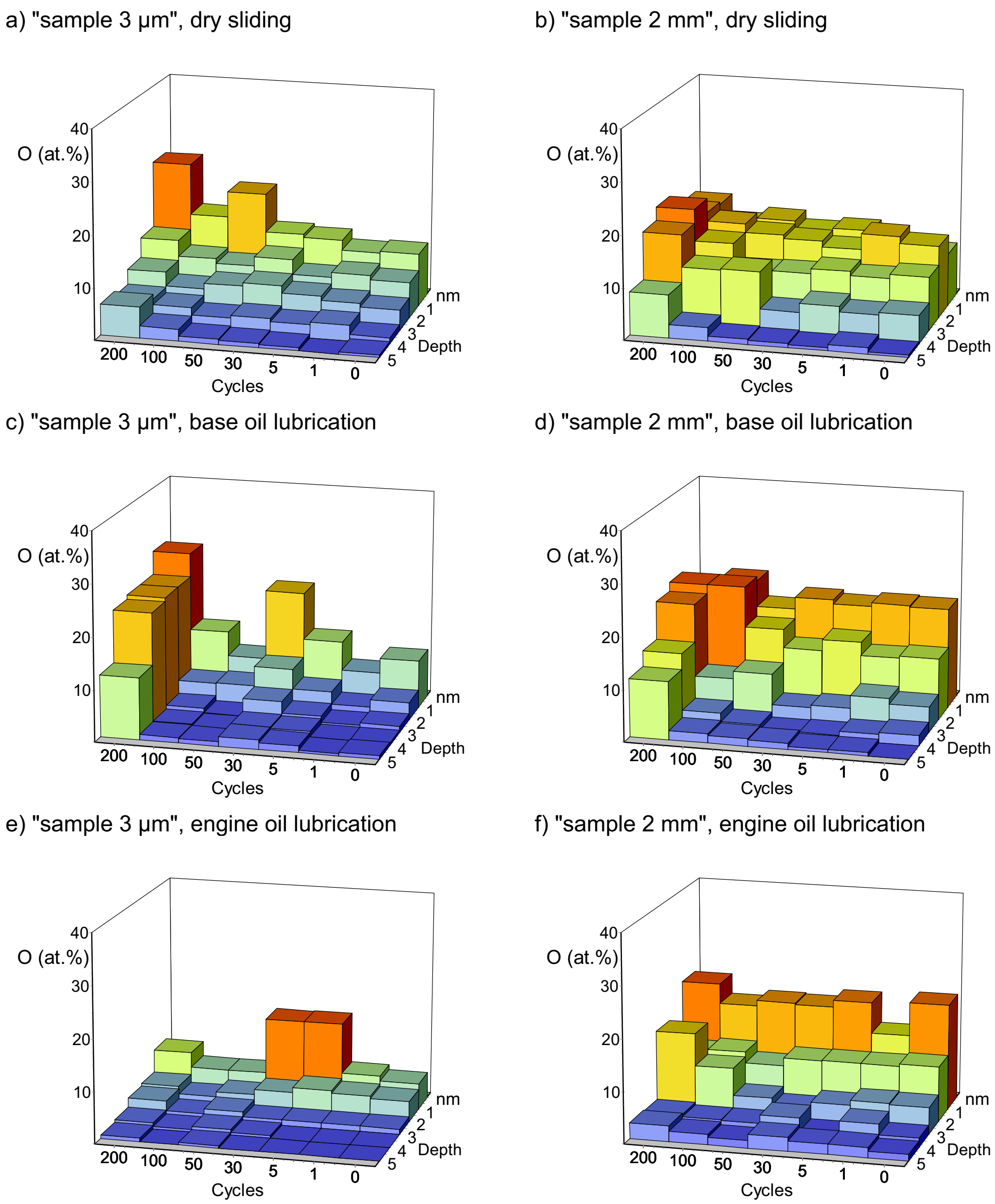

Fig. 8. Atomic concentration of oxygen in the wear tracks as obtained with Auger electron spectroscopy.

4 Discussion

4.1 On the microscopic scale

We would like to discuss the results with the mechanistic prospective on friction given in references [2] and [1]. In these works the friction force was expressed in terms of a deformation force F_{def} and boundary lubrication force F_{BL}:

$$F_{\mathrm{R}} = F_{\mathrm{def}} + F_{\mathrm{BL}}. \tag{2}$$

The deformation part F_{def} of the friction force is a function of the mechanical properties of the material and the volume that is plastically deformed. The part F_{BL} represents the boundary lubrication as dissipation channel and is a

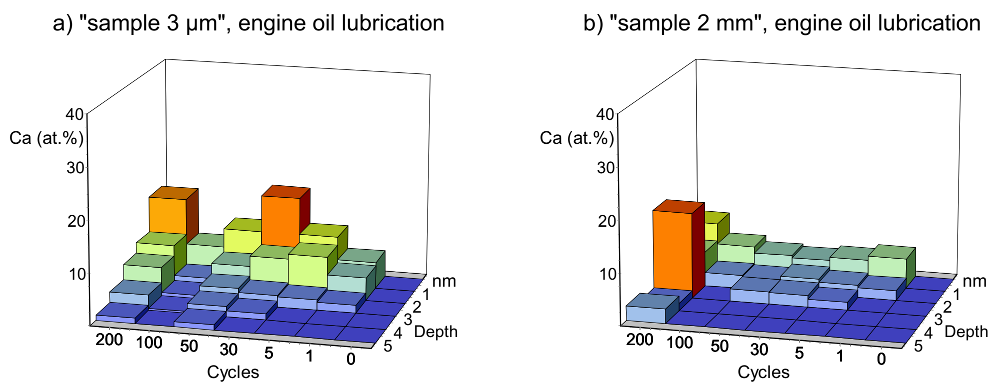

Fig. 9. Atomic concentration of calcium in the wear tracks as obtained with Auger electron spectroscopy.

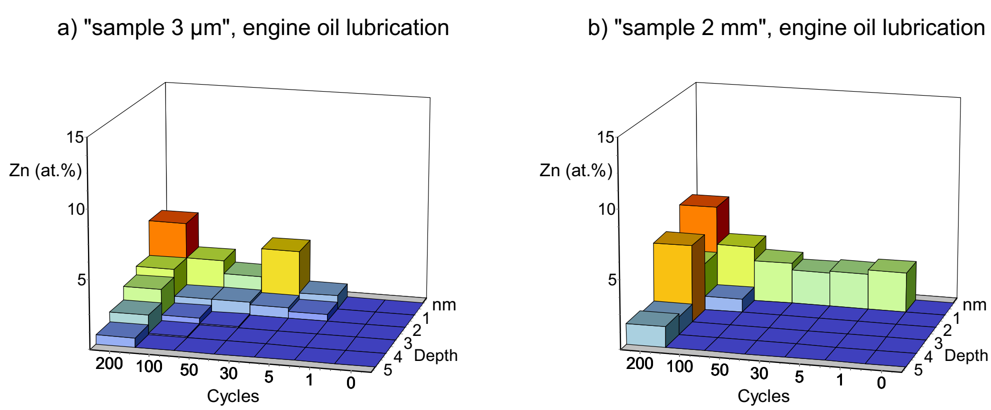

Fig. 10. Atomic concentration of zinc in the wear tracks as obtained with Auger electron spectroscopy.

function of the sliding area and the shear modulus of the interface. We subclassify the running time of the system using the obtained results into periods which are independent of the initial structure of the sample.

(1) 1-2 cycles: Intensive plastic deformation occurs due to high stress, which is consequence of the small contact area. The real contact area is equal to the nominal contact area (saturated plastic contact). The area A_2 increases rapidly and wedge formation occurs. In the initial part F_{def} dominates F_{BL}.
(2) 2-50 cycles: The real contact area is still equal to the nominal contact area, but only some regions are involved into plastic deformation (transition: saturated elastoplastic contact - unsaturated elastoplastic contact). The portion of plastic contact and the wear rate decrease. The part of boundary lubrication increases slightly for dry lubrication and strongly for lubricated surfaces due to the larger interface area. The total friction force decreases for dry friction and decreases slightly for lubricated friction depending on the type of oil used.
(3) 50-200 cycles: The real contact area is no longer equal to the nominal contact area. Plastic deformation occurs in a few regions of contact (unsaturated elastoplastic contact). The interface area, shear modulus of the interface and, hence, the boundary lubrication part of friction force depend on the type of oil. F_{BL} is dominating, but a small portion of plastic deformation is still present.

In framework of the classification given above, during the period 1, the diamond sphere is introduced deeper into the "sample 2 mm" than into the "sample 3 μm" due to the lower yield strength of the latter surface. The necessity to deform larger volume causes higher friction and a higher wear rate of "sample 2 mm" during this period. In the period 2, the friction of both samples is very similar, but not the wear rate. "Sample 2 mm" is slighly less

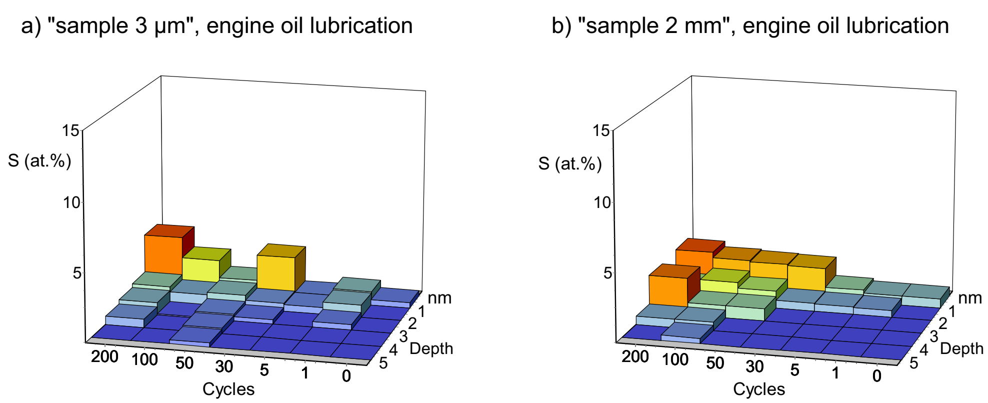

Fig. 11. Atomic concentration of sulphur in the wear tracks as obtained with Auger electron spectroscopy.

wear resistant than "sample 3 μm". Larger β_{HK} on "Sample 2 mm" during periods 1 and 2 lessen the support from the wedges on the latter period 3 causing slightly higher contact pressure. The initial microstructure of the Cu sheet is changing significantly until the 50th cycle (see Figs. 5 and 6) and only slightly afterwards. Texture, which appears in sliding direction due to intensive deformation, remains for short time. The sample recrystallizes slightly under a low friction in period 3, as is shown by the EBSD investigation (see Fig. 7). The initial grain size does not affect this process significantly.

As shown by the friction results, lubrication leads to an increase of the friction coefficient particularly in period 3. The increase of friction is a consequence of addition of viscous and boundary forces of the oil. Such significant increase of friction due to an addition of a fluid into the contact is well-known in microtribology, but also was shown by Bowden and Tabor [2] in a macroscopic system, at low normal loads and sliding velocities. Naturally the higher increase of friction is with lubrication with engine oil because of higher viscosity.

Wear of "sample 3 μm" is not affected by the lubrication. It meets the expectation because the antiwear additives are not designed to work at such low temperatures [25] and soft surfaces such as Cu [26]. A relatively high sensitivity to the kind of lubrication in case of "sample 2 mm" was indicated by β_{HK} during the "steady state" period. The significant change of interaction of the diamond sphere with Cu was due to brittle destruction of natural oxide layer of Cu by diamond sphere (secondary abrasion). Some pieces of hard oxide layer adhered on diamond and consequently produced additional grooves inside of the initial wear track. Such effect occurred in all three repetitions of test series under dry sliding, but the introduction of lubricant changed the contact mechanics and eliminated this effect. In the case of "sample 3 μm" there is no evidence for secondary abrasion, which is connected with by factor 1.5 higher bulk hardness of this sample.

Chemical modification of surface regions seem to be independent on the initial grain size. It is known that due to oscillated mechanical stress and plastic flow diffusion can be accelerated significantly [27,28]. In our experiments, however, plastic flow during the periods 1 and 2 plays a big role. No significant change in the elemental composition was found (see Figs. 8, 9, 10, and 11). The main reason for such behaviour is the high wear rate during periods 1 and 2. The chemically modified material is transferred to the shoulders or ends of the track. Analysis of material on the shoulders of the wear track confirmed low concentration of Cu and major presence of oxygen and lubricant components. Thus, changes (max. depth about 8 nm) of the chemical composition of near-surface regions in wear tracks become obvious after 200 cycles. Elements involved into the near-surface regions come from the environment depending on the kind of lubrication. Under dry friction conditions, the oxidation is the main process of the chemical modification.

Running-in in a microscopic system is useful in the description of such process in the macroscopic scale because of similarity of friction and wear as function of time. The first period of the running-in is characterized by intensive plastic flow due to small contact area and, hence, large stress. Therefore decrease of grain size occur. The adjustment of macroscopic topography of counter parts happens as well as the modification of the surface's mechanical properties due to plastic flow (e.g; work hardening). The Hall-Petch relation [29,30] could be used to identify change of mechanical properties since only slight changes of chemistry of the surface occur due to high wear rate. In other words, the rate of chemical modifications (incorporation of elements into surface or chemical reaction) does not cover the rate of removal of the material out of the contact. The period of extensive plastic deformation in a macroscopic system, usually is substantially greater than in the microscopic (2 sliding interactions in microscopic system versus around 500 in macroscopic [5] pp. 266), because the asperities of a rough technical surface are not permanently in contact with same asperities of the counter surface. Nevertheless such period of severe plastic deformation is short compared to the service life of the system, it has a major influence on further function of tribosystem for the following reasons:

(1) the wear rate during running-in is by factor $> 10^2$ higher than the one during "steady state" period and could produce significant wear amount affecting the function of the system
(2) the "chance" to have the highest level of plastic deformation localized in the near surface region is given only once - if the surfaces are unworn or "unadjusted".

From this point of view the running-in period could influence the function of the system during further operating time, if the wear rate is low to wear out the modified (e.g. plastically deformed) surface zones.

The "steady state" period of wear and friction should represent the equilibrium between the minor decrease and increase of grain size. The boundary and viscous properties of the lubricant and surfaces play then a major role. Regarding the chemical modification of the surface due to friction, we showed that the depth of chemical modification is coupled with amount of local interactions (cycles).

Some aspects such as the lubricant's influence on grain size evolution, or the influence of the initial grain size on the depth of chemical modification should be investigated more detailed under variation of the temperature in the contact. In the microscopic tribosystem these processes seem to be unconnected at low temperature. Another topic is the more accurate investigation of grains shape of near surface regions. Further works are in progress to obtain three-dimensional structural information.

5 Summary

This study deals with the influence of the initial grain size of the softer of two tribopartners on the running-in related phenomena. A microscopic tribosystem diamond sphere / Cu sheet was tested under dry and lubricated reciprocated sliding. The gradual changes of the microstructure and the chemical composition of the Cu surface during friction are investigated according to the measurement of the coefficient of friction and wear rate.

It is shown that first interactions of unworn surfaces are accompanied by an extensive plastic flow which induces the grain size reduction. The grains reach a size of about 500 nm independent of the initial grain size with a texture in sliding direction. First sliding interactions determine the wear of the system significantly. The softer Cu with larger grains therefore has higher wear and, especially under dry sliding, a higher friction coefficient than the Cu sample with initially small grains.

After the period with extensive plastic deformation, the influence of the initial structure on friction is minimized because of modification and unification of the structure near the surface. The boundary lubrication is dominating. Thus, a slight recrystallization can occur. Chemical changes of the surface occur intensively due to operating with low wear rate. The depth of chemical changes is determined significantly by the amount of interactions. In the microscopic system chemical modification could be 8 nm deep after 200 reciprocations.

Acknowledgements

The authors are grateful to T. Ditz from the Institut für Materialforschung IMF II, Forschungszentrum Karlsruhe GmbH, for the measurement of hardness and Young's modulus profiles of Cu samples. We also thank L. Echtle for help in preparing the Cu samples and acknowledge M. H. Müser for very helpful discussion.

References

[1] I. Kragelsky, M. Dobychin, V. Kombalov, Friction and wear, calculation methods, Pergamon Press, Oxford, 1982.

[2] F. Bowden, D. Tabor, The friction and lubrication of solids, Clarendon Press, Oxford, 1950.

[3] P. J. Blau, Friction and wear transitions of materials, Noyes Publications, Park Ridge, NJ, 1989.

[4] B. Kehrwald, Untersuchung der Vorgänge in tribologischen Systemen während des Einlaufs, PhD thesis, University Karlsruhe, 1998.

[5] P. Blau, Friction Science and Technology, 1st Edition, Marcel Dekker, Amsterdam, 1996.

[6] J. P. Rigney, D. A.; Hirth, Plastic deformation and sliding friction of metals, Wear 53 (1979) 345–370.

[7] L. K. I. Doris Kuhlmann-Wilsdorf, Subsurface hardening in erosion-damaged copper as inferred from the dislocation cell structure, and its dependence on particle velocity and angle of impact, Wear 85 (1983) 361–373.

[8] J. L. YoungJr, D. Kuhlmann-Wilsdorf, R. Hull, The generation of mechanically mixed layers (mmls) during sliding contact and the effects of lubricant thereon, Wear 246 (2000) 74–90.

[9] M. S. Bednar, D. Kuhlmann-Wilsdorf, Amorphous and alloy film formation in sliding of silver on copper, Wear 181-183 (1995) 922–937.

[10] P. Blau, Investigation of the nature of micro-indentation hardness gradients below sliding contacts in five copper alloys worn against 52100 steel, Journal of Materials Science 19 (6) (1984) 1957–1968.

[11] S. L. Rice, H. Nowotny, S. F. Wayne, Characteristics of metallic subsurface zones in sliding and impact wear, Wear 74 (1981) 131–142.

[12] R. K. S. M. Rigney, D. A.; Divakar, Deformation substructures associated with very large plastic strains, Scripta Metallurgica et Materialia 27 (1992) 975–980.

[13] D. Shakhvorostov, B. Gleising, R. Bscherb, W. Dudzinski, A. Fischer, M. Scherge, Microstructure of tribologically induced nanolayers produced at ultra-low wear rates, Wear .

[14] J. Schiøtz, F. Di Tolla, K. Jacobsen, Softening of nanocrystalline metals at very small grain sizes, Nature 391 (1998) 561.

[15] E. Arzt, Size effects in materials due to microstructural and dimensional constrains: a comparative review, Acta Mater. 46 (1998) 5611–5626.

[16] D. Shakhvorostov, K. Phlmann, M. Scherge, Structure and mechanical properties of tribologically induced nanolayers, Wear 260 (2006) 433–437.

[17] N. Ohmae, T. Tsukizoe, F. Akiyama, On the microscopic processes involved in metallic friction, Philosophical Magazine A 40 (6) (1979) 803–810.
URL http://www.informaworld.com/10.1080/01418617908234875

[18] T. El-Raghy, P. Blau, M. Barsoum, Effect of grain size on friction and wear behavior of Ti_3SiC_2, Wear 238 (2) (2000) 125–130.

[19] G. Bregliozzi, A. Di Schino, H. Kenny, J.M. Haefke, Influence of atmospheric humidity and grain size on the friction and wear of high nitrogen austenitic stainless steel, Journal of Materials Science 39 (4) (2004) 1481–1484.

[20] M. Scherge, S. N. Gorb, Biological Micro- and Nanotribology. Nature's Solutions, Springer, Berlin, 2001.

[21] T. Kayaba, K. Hokkirigawa, K. Kato, Analysis of the abrasive wear mechanism by successive observations of wear processes in a scanning electron microscope, Wear 110 (1986) 419–430.

[22] K. Zum Gahr, Microstructure and wear of materials, Elsevier, Amsterdam, 1987.

[23] A. Czanderna, Methods of surface analysis, Vol. 1, 1st Edition, Elsevier, Amsterdam, 1975.

[24] D. Watson, Improved dynamic range and automated lineshape differentiation in aes/xps composition versus depth profiles, Surface and Interface Analysis 15 (9) (1990) 516–524.

[25] M. I. De Barros, J. Bouchet, I. Raoult, T. Le Mogne, J. M. Martin, M. Kasrai, Y. Yamada, Friction reduction by metal sulfides in boundary lubrication studied by XPS and XANES analyses, Wear 254 (9) (2003) 863–870.

[26] N. J. Mosey, M. H. Müser, T. K. Woo, Molecular mechanisms for the functionality of lubricant additives, Science 307 (2005) 1612 – 1615.

[27] D. A. Rigney, Transfer, mixing and associated chemical and mechanical processes during the sliding of ductile materials, Wear 245 (2000) 1–9.

[28] G. Heinicke, Tribochemistry, Hanser Verlag, München, 1984.

[29] E. O. Hall, The deformation of mild steel. III. Discussion of results, Proc. Phys. Soc. B 64 (1951) 747.

[30] N. J. Petch, The cleavage strength of polycrystals, J. Iron Steel Inst. 174 (1953) 25.